

## **Antiangiogenic liposomal gene therapy with 16K human prolactin efficiently reduces tumor growth.**

Virginie Kinet<sup>1</sup>, Ngoc-Quynh-Nhu Nguyen<sup>1</sup>, Céline Sabatel<sup>1</sup>, Silvia Blacher<sup>2</sup>, Agnès Noël<sup>2</sup>, Joseph A Martial<sup>1</sup> and Ingrid Struman<sup>1</sup>

<sup>1</sup> GIGA-Research, Molecular Biology and Genetic Engineering Unit, University of Liège, Belgium;

<sup>2</sup> GIGA-Research, Laboratory of Tumor and Development Biology, University of Liège, Belgium

### **Abstract**

Human 16K PRL (16K hPRL) is a potent inhibitor of angiogenesis both *in vitro* and *in vivo*. It has been shown to prevent tumor growth in three xenograft mouse models. Here we have used a gene transfer method based on cationic liposomes to produce 16K hPRL and demonstrate that 16K hPRL inhibits tumor growth in a subcutaneous B16F10 mouse melanoma model. Computer-assisted image analysis shows that 16K hPRL treatment results in the reduction of tumor vessel length and width, leading to a 57% reduction in average vessel size. We thus show, for the first time, that administration of the 16K hPRL gene complexed to cationic liposomes is effective to maintain antiangiogenic activities of 16K hPRL level.

*Keywords:* antiangiogenic therapy; 16K hPRL, cationic liposomes; transfection

### **1. Introduction**

Angiogenesis, the formation of new blood vessels from pre-existing ones, is essential to organ growth and repair. An imbalance in this process contributes to the pathogenesis of numerous disorders, notably cancer[1]. Angiogenesis is a multi-step process including endothelial cell proliferation, migration, basement membrane degradation, and new lumen organization. Within a given microenvironment, the angiogenic response is regulated by a balance between pro- and anti-angiogenic regulators[2]. Induction of a tumor vasculature, termed the “angiogenic switch”, occurs when this balance tips in favor of pro-angiogenic factors[3]. The role of angiogenesis in tumor growth and progression being firmly established, considerable efforts have focused on antiangiogenic therapy as a new form of cancer treatment[2], especially since angiogenesis inhibitors have two advantages: they are less toxic than conventional chemotherapy and entail a lower risk of drug resistance[4]. Antiangiogenic therapy is now considered as an effective approach for cancer therapy, indeed FDA-approved antiangiogenic therapies in oncology.

There are currently eight approved anti-cancer therapies with recognized antiangiogenic properties. These agents, which interrupt critical cell signaling pathways involved in tumor angiogenesis and growth, comprise two primary categories: 1) monoclonal antibodies directed against specific proangiogenic growth factors and/or their receptors (examples: Avastin®, Herceptin®); and 2) small molecule tyrosine kinase inhibitors (TKIs) of multiple proangiogenic growth factor receptors (examples: Tarveca®, Nexavar®). Inhibitors of mTOR (mammalian target of rapamycin) represent a third, smaller category of antiangiogenic therapies with one currently approved agent. In addition, at least two other approved angiogenic agents may indirectly inhibit angiogenesis through mechanisms that are not completely understood.

16K PRL, the 16-kDa N-terminal fragment of prolactin, is a potent negative regulator of angiogenesis. We have previously shown that it is antiangiogenic both *in vitro* and *in vivo*[5-12]. Very recently, human 16K PRL (16K hPRL) was shown to play a role in postpartum cardiomyopathy[13]. Its antitumor activity has been demonstrated in three mouse models. Bentzien and collaborators have shown that 16K hPRL, produced by human HCT116 colon

cancer cells, markedly reduces their ability to form subcutaneous (s.c.) tumors in *Rag1*<sup>-/-</sup> mice[14]. Moreover, by using an adenovirus vector as gene transfer method for 16K hPRL, Kim and collaborators and also Nguyen and collaborators, have respectively shown that the expression of 16K hPRL in prostate cancer cells leads to tumor growth inhibition and that 16K hPRL inhibits tumor growth in a s.c. B16F10 mouse melanoma model and reduces the establishment of B16F10 metastasis in an experimental lung metastasis model[15,16].

There are obstacles to carrying out clinical trials of antiangiogenic protein therapy: prolonged protein therapy, repeated administration, high dosages, toxicity risks, and high cost. To overcome these problems, it is thus necessary to develop alternative strategies. Antiangiogenic gene therapy has become one of the most attractive approaches to the treatment of cancer[17]. In particular, non-viral delivery of the payload gene via “lipoplexes” (complexes of cationic liposomes and plasmid DNA) has become popular in both *in vitro* and *in vivo* research in this field. Liposomal vectors offer clear advantages over recombinant viral vectors: they are non-pathogenic and less immunogenic; they impose no limit on transgene size and are simple to prepare and use. Cationic liposomes appear particularly suitable for antiangiogenic antitumor therapy, as Thurston and his collaborators have shown in a mouse system that they target mainly tumoral blood vessels[18]. Maeda and collaborators have also shown that liposomes tend to accumulate in tumor tissues through the angiogenic endothelium via the enhanced permeability and retention effect[19]. For these reasons, cationic liposomes have been used as safe vehicles for gene transfer in a variety of gene therapy clinical trials, and notably in antiangiogenic gene therapy[20-22].

In this study we have investigated the effect of 16K hPRL on primary tumor development from B16F10 murine melanoma cells. We provide evidence that 16K hPRL, administered by cationic-liposome-mediated gene transfer, can reduce tumor growth by altering the vascular morphology of tumors.

## **2. Materials and Methods**

### **2.1. Cell lines, animals, and reagents**

Transformed human kidney cells (293T cells) were cultured in DMEM 1000 (50%) and HAM F12 (50%) supplemented with 10% FBS and antibiotics (100 units/ml penicillin and 100µg/ml streptomycin) at 37 °C in a humid atmosphere containing 5% CO<sub>2</sub>. B16F10 mouse melanoma cells were obtained from the American Type Culture Collection (ATCC CRL-6475, Rockville, Md) and cultured in DMEM 4500 supplemented with 10% FBS and 100 units/ml penicillin, 100µg/ml streptomycin at 37 °C in a humid atmosphere containing 5% CO<sub>2</sub>. All culture reagents were purchased from Invitrogen Corp./Life Technologies (CA, USA). Adult female C57BL/6J mice (6-8 weeks of age) purchased from the Central Animal Facility of CHU Liège (Liège, Belgium) were used to assess tumor growth.

DOTAP (1,2-Dioleoyl-3-trimethylammonium propane) and cholesterol were purchased from Avanti Polar Lipids, Inc (Alabaster, AL, USA). Lipofectamine reagent was purchased from Invitrogen Corp./Life Technologies (CA, USA).

### **2.2. DNA preparation**

Plasmids pcDNA3.1-16K hPRL and pcDNA3.1 were amplified and purified with the EndoFree Plasmid Megaprep Kit (QIAGEN, Hilden, Germany). This kit makes it possible to remove endotoxin.

### **2.3. Cationic liposome synthesis**

DOTAP and cholesterol (1:1 w/w) were mixed and dissolved in chloroform/methanol (1:1 v/v). The solution was evaporated under vacuum in a rotary evaporator until a thin lipid film was formed. The lipids were kept under vacuum overnight to ensure removal of the residual organic solvent. The following day, the dried lipid film was hydrated with 2 ml phosphate-buffered saline (PBS) to form multilamellar liposomes. The suspension was left for 2 hours to allow swelling of the liposomes. 5 cycles of freezing under N<sub>2</sub>/thawing at 37 °C were performed to weaken the membrane lipids. Finally, an extruder (Polar Lipids, Inc. Alabaster, AL, USA) was used to extrude the suspension 10 times through polycarbonate filters (pore size: 100 nm). The liposomes were stored at 4 °C.

#### **2.4. Preparation of DNA:liposome complexes (lipoplexes)**

For *in vitro* gene transfection, 100 (or 50) µg liposomes (or lipofectamine) were diluted in 250 µl Optimem, and 10 (or 5) µg plasmid DNA was also diluted in 250 µl Optimem. The resulting mixtures were mixed and incubated at room temperature for 30 minutes to form stable DNA:liposome complexes. For *in vivo* transfection, an equal volume of plasmid DNA solution was added to the liposome solution by slow dropwise addition with continuous mixing to achieve a 1:10 DNA:lipid ratio (by weight). The resulting lipoplexes were incubated at room temperature for 30 minutes before administration to mice.

#### **2.5. Western blot analysis**

37.5 µl from conditioned medium of 293T cells transfected with lipoplexes containing cationic liposomes (100 µg) and pcDNA3.1 or pcDNA3.1-16K hPRL (10 µg) was resolved by SDS-PAGE and transferred to a polyvinylidene fluoride membrane (Millipore Corp., Bedford, MA, USA). Membranes were saturated for 1 hour in TBS-8% dry milk, followed by incubation for 1 hour with a 1/500 dilution of anti-16K hPRL antibody (A602) and for 1 hour with a 1/5000 dilution of peroxidase-conjugated goat antirabbit antibody (Gamma, BioWhittaker, Verviers, Belgium). 16K hPRL detection was done by chemiluminescence with the ECL Plus Kit (Amersham Biosciences, Arlington Heights, IL, USA). For the deglycosylation experiments, the N-Glycosidase F Deglycosylation Kit was used according to the manufacturer's instructions (Roche, Palo Alto, CA) as previously described[23].

#### **2.6. qRT-PCR**

Total RNA was extracted from 30 mg tumor tissue with MagNA Lyser Green Beads according to the manufacturer's instructions (Roche Applied Science, Mannheim, Germany). RNA was isolated with the Qiagen Rneasy Mini kit (Qiagen, Hilden, Germany) and treated with Dnase (RQ1 RNase-Free Dnase, Promega, Madison, WI). cDNA was synthesized from 1 µg total RNA by reverse transcription with the RT Transcriptor First Strand cDNA Synthesis Kit (Roche Clinical Laboratories, Indianapolis, IN) according to the manufacturer's instructions. The resulting cDNA (300 pg) was used for real-time PCR with the one-step 2x Mastermix (Diagenode, Liège, Belgium) containing SYBR green. Thermal cycling was performed on an Applied Biosystems 7000 detection system (Applied Biosystems, Foster City, CA). For all reactions, negative controls were run with no template present, and random RNA preparations were also subjected to sham qRT-PCR (no reverse transcription) to verify lack of genomic DNA amplification. The relative transcript levels for the genes of interest were obtained by the relative standard curve method and normalized with respect to the housekeeping gene cyclophilin B. Primers, the sequences of which are available upon request, were designed with the Primer Express 2.0 software (Apply Biosystem, Forster City, USA) and selected so as to span exon-exon junctions, to avoid detection of genomic DNA.

#### **2.7. In vitro transfection**

293T cells were seeded into 10-cm plates at a density of  $4.5 \times 10^6$  cells per plate. 24 hours later, the medium was replaced with serum-free medium and then prepared lipoplexes were added to the culture plates (10  $\mu$ g DNA per plate), which were then incubated at 37 °C in 5% CO<sub>2</sub> for 4 hours. The transfected cells were incubated for another 48 hours in the presence of serum-containing medium.

### **2.8. *In vivo* gene transfection**

Subconfluent B16F10 were trypsinized, washed, and resuspended in PBS. Cell suspension (10<sup>5</sup> cells in 50  $\mu$ l) was injected s.c. into the right flanks of C57BL/6J mice. Experimental groups of twelve mice were used and randomly divided. Three days later, prepared lipoplexes (50  $\mu$ g plasmid DNA/500  $\mu$ g cationic liposomes) were inoculated s.c. into the peritumoral region. This injection was repeated every three or four days. Eighteen days after cell injection, the mice were sacrificed and tumors harvested. Tumor growth was assessed by measuring the length and width of each tumor every one or two days and calculating its volume by means of the formula: length x width<sup>2</sup> x 0.5. Results are expressed as the mean tumor volume for each experimental group.

### **2.9. Histology and immunohistochemistry**

Tumors were embedded in Tissue-Tek (Sakura Finetek, Zoeterwoude, The Netherlands) and frozen at -70 °C prior to sectioning (into slices 5  $\mu$ m thick). To study overall tissue morphology, frozen sections were stained with hematoxylin/eosin. For assessment of angiogenesis, tumor vessels were stained with CD31. For CD31 staining, frozen sections were fixed in 80% MetOH (VWR, Leuven, Belgium) for 10 minutes at -20 °C. Endogenous peroxidase was subsequently blocked with 3% H<sub>2</sub>O<sub>2</sub>/H<sub>2</sub>O (Sigma-Aldrich, Steinheim, Germany) for 20 minutes, and non-specific binding was prevented by incubation in normal rabbit serum for 1 hour at room temperature. Sections were then incubated first with a rat monoclonal anti-CD31 (1/250, BD Biosciences, Erembodegem, Belgium) for 1 hour at room temperature, then with a biotinylated secondary antibody (1/400, DAKO, Heverlee, Belgium) for 30 minutes at room temperature. This was followed by incubation with streptavidin/HRP complex (1/500, DAKO, Heverlee, Belgium). CD31-positive cells were visualized after sections were colored for 3 minutes with 3-amino-9-ethylcarbazole (DAKO, Heverlee, Belgium). Sections were finally counterstained with hematoxylin and mounted for microscopy with Aqua Polymount (Polysciences Inc., Warrington, PA, USA).

### **2.10. Image processing and measurements**

Images were digitized in 1360 x 1024 pixels in the red-green-blue (RGB) color space. Image processing and measurements were performed with the software Aphelion 3.2 from Adsis (France) on a PC as described previously[16]. Briefly, 15 images, including a total of about 500 vessels, were analyzed for each condition. Immunostaining of histological tumor sections for CD31 makes it possible to distinguish tumor vessels from tissue. The red component of the RGB color image corresponding to vessels was first extracted and the resulting image was further processed. The following measurements were performed:

- (a) Vessel density defined as the number of vessels per unit of tissue area
- (b) Area density defined as the percentage of tissue area occupied by vessels
- (c) Vessel size distribution.

### **2.11. Statistical analysis**

All data are expressed as means  $\pm$  SME. Analyses for statistical significance (the Mann-Whitney test) were carried out with Prism 4.0 software (GraphPad Software, San Diego, CA, USA). Statistical significance was set at  $P < 0.05$ .

### **3. Results**

#### **3.1. Transfection with cationic liposomes composed of DOTAP and cholesterol**

To check whether cationic liposomes composed of DOTAP and cholesterol allow efficient transfection *in vitro*, we used them to transfect 293T cells, a cell line known to be efficiently transfectable by liposomes. The cells were treated with lipoplexes consisting of cationic liposomes and pCMTEGFP (a plasmid allowing eGFP expression). For comparison, transfection with lipofectamine and pCMTEGFP was also included. 24 hours after treatment, the cells were analyzed by fluorescence microscopy. The results show that cationic liposomes are very efficient transfer gene vectors. The comparison with lipofectamine points out that cationic liposomes are as efficient as even more lipofectamine (Fig 1).

#### **3.2. Cationic liposomes allow expression of 16K hPRL *in vitro***

The ability of cationic liposomes to allow 16K hPRL expression was assessed *in vitro* with the 16K hPRL-encoding plasmid pcDNA3.1-16K hPRL. 293T cells were treated with lipoplexes composed of cationic liposomes (50 µg) and pcDNA3.1-16K hPRL or pcDNA3.1 (5 µg). After 48 hours of transfection, the culture medium was collected and assayed by immunoblotting. Immunostaining with anti-16K hPRL antibody revealed 16K hPRL expression (Fig 2a). Western blot analysis revealed a band running higher than that seen for recombinant 16K hPRL produced in *Escherichia coli* (Fig 2a). This is due to the N-glycosylation of Asn 31 of 16K hPRL. Deglycosylation of the cell culture medium with N-glycosidase F revealed a band co-migrating with the recombinant 16K hPRL made in *E. coli* (Fig 2b), as previously shown[23].

#### **3.3. 16K hPRL expression by cationic liposomes inhibits tumor growth in a mouse model**

The effect of 16K hPRL on solid tumor growth was assessed in a mouse model of B16F10 melanoma. 10<sup>5</sup> B16F10 cells were subcutaneously injected into C57BL/6J mice. Two groups of twelve mice were used. One group was treated peritumorally every three to four days with lipoplexes consisting of cationic liposomes (500 µg) and plasmid pcDNA3.1-hPRL 16K (50 µg) and the other group was treated similarly with lipoplexes consisting of cationic liposomes (500 µg) and control plasmid pcDNA3.1 (50 µg). Tumors grown in 16K hPRL-treated mice displayed a volume significantly smaller than the tumors of the control group (Fig 3). We monitored the effect of 16K hPRL on tumor growth in two independent experiments. In both experiments, tumor growth was reduced in the mouse groups treated with 16K hPRL.

#### **3.4 The 16K hPRL gene is expressed in B16F10 tumors**

The 16K hPRL mRNA level was assessed in mouse tumors treated with plasmid pcDNA3.1-16K hPRL or pcDNA3.1 by quantitative RT-PCR performed on cDNA samples prepared by reverse transcription from mouse-tumor RNA extracts. Figure 4 shows that 16K hPRL mRNA was detected at a high level in tumors from mice treated with plasmid pcDNA3.1-16K hPRL.

#### **3.5 Modification of vascular morphology by 16K hPRL**

Considering the previously described ability of 16K hPRL to alter tumoral vasculature[16], we used anti-CD31 antibodies to immunostain tumor blood vessels in sections obtained from both groups of mice. We observed interesting differences in tumor-vessel morphology and size between the two groups, the blood vessels appearing smaller and collapsed in tumors treated with 16K hPRL (Fig 5a). Computer-assisted image analysis was used to quantify vessel density (number of CD31-positive vessels per µm<sup>2</sup> tumor area), vessel area density (percentage of the tumor area occupied by blood vessels), and vessel size distribution (Fig 5b-

e). Although the average vessel density was similar in the two groups (Fig 5b), the vessel area density was smaller in the 16K hPRL-treated mice (Fig 5c). This was due to the smaller length and width of blood vessels in the 16K hPRL-treated tumors than in the control tumors, resulting in a 57% reduction in blood vessel size (Fig 5d). Accordingly, the vessel size distribution histogram (Fig 5e) shows a reduction in the number of vessels above 2000  $\mu\text{m}^2$  in size after treatment with 16K hPRL. These results confirm that the antiangiogenic factor 16K hPRL can reduce the development of B16F10 melanoma by altering tumor vasculature.

#### **4. Discussion**

Angiogenesis, the formation of new blood vessels from pre-existing ones, is a phenomenon intervening in several physiological and pathological processes[1]. In 1971, Dr. Judah Folkman first proposed that tumor growth is angiogenesis-dependent[24]. Activation of tumoral angiogenesis is due to an imbalance between pro- and anti-angiogenic factors. Bouck and his collaborators have thus proposed the “angiogenic switch” model to explain tipping of the balance in favor of pro-angiogenic factors[25]. Angiogenesis has thus become a therapeutic target of great interest in cancer research.

Among antiangiogenic factors, 16K hPRL appears as an interesting candidate. The antitumoral effect of 16K hPRL has already been evaluated in three murine models[14,16,21]. In these studies, 16K hPRL was produced either by injected tumor cells transformed beforehand *in vitro* with an appropriate expression vector or from an adenoviral vector injected at the site of nascent tumors. Here, we have evaluated the antitumor effect of 16K hPRL in a murine system after non-viral transfer of the 16K hPRL-encoding gene. For this we have used cationic liposomes to induce the expression of 16K hPRL in the environment of B16F10 melanoma tumoral cells established subcutaneously in the right flanks of C57BL/6J mice. We chose to use B16F10 cells because they are highly invasive, and four major reasons justified our choice of cationic liposomes as gene carriers. Firstly, cationic liposomes are non-immunogenic, unlike viral vectors. Secondly, they can be produced easily and in large quantity. Thirdly, their positive charges interact electrostatically with the negative charges of DNA and they preferentially target tumoral blood vessels. Lastly, many experiments have proven the efficiency of cationic liposomes as gene transfer vehicles[20,21,26,27]. Here we have demonstrated this efficiency *in vitro* with the plasmid allowing expression of eGFP.

On the basis of tumor volumes measured in mice treated with pcDNA3.1- 16K hPRL or pcDNA3.1, we clearly show that 16K hPRL administered in this way can reduce tumor growth. These results validate both cationic liposomes as efficient gene vehicles *in vivo* and the use of the antiangiogenic factor 16K hPRL as an antitumor agent in our mouse model. Furthermore, in keeping with the observation of Nguyen and her collaborators that the antitumor activity of 16K hPRL in a subcutaneous tumor model is associated with an effect on tumor blood vessel morphology[16], our CD31 immunostaining data show that the tumor vessels are smaller and more collapsed following 16K hPRL treatment. This observation is corroborated by computer-assisted image analysis revealing a 57% decrease in the average vessel area in pcDNA3.1- 16K hPRL-treated than in pcDNA3.1-treated tumors. As suggested by Nguyen, 16K hPRL could be having an effect on vascular tone. Indeed 16K hPRL is known to inhibit eNOS activation by blocking intracellular  $\text{Ca}^{2+}$  mobilization, and this action results in inhibition of both angiogenesis and vasorelaxation[28].

In conclusion, this study again underlines the ability of 16K hPRL to inhibit tumor growth efficiently in a mouse model, this inhibition being mediated by an effect of 16K hPRL on tumor blood vessel morphology. Our results also highlight liposome-mediated gene therapy as a promising alternative to protein therapy.

#### **Conflicts of interest statement**

All authors declare that they do not have any conflicts of interest.

## **Acknowledgments**

The authors thank Christelle Flore and Laurence Lins (Center of Numerical Molecular Biophysics, Gembloux) for assistance in liposome preparation, Isabelle Dasoul (Laboratory of Tumor and Developmental Biology) for immunohistochemical staining and Michelle Lion for her excellent technical assistance. This work was supported by grants from the Fonds pour la Recherche Industrielle et Agricole (FRIA) (to VK, CS), the Fonds National de la Recherche Scientifique (FNRS) (to IS) and the program NEOANGIO from the “region wallonne”.

## **Titles and legends to figures**

**Figure 1** Comparison of transfection efficiencies of cationic lipoplexes and lipofectamine in 293T cells. For both transfection vehicles the same amount of DNA (pCMTEGFP = 10 µg) was used. Cationic liposomes (equivalent to 100 µg lipid) were composed of a DOTAP/cholesterol mixture at a molar ratio 1:1. Lipofectamine (equivalent to 100 µg lipid) was used as instructed by the manufacturer. Analyses were performed under a fluorescence microscope (x100 magnification).

**Figure 2** Cationic liposomes allow *in vitro* expression of 16K hPRL. **(a)** Transfection of 293T cells with a plasmid encoding 16K hPRL was carried out in 100-mm plates with the help of DOTAP/cholesterol cationic liposomes. After 48h of incubation, the cell culture media were subjected to SDS-PAGE and then analysed by western blotting with an anti-16K hPRL antibody. *Lane 1*; 30 ng recombinant 16K hPRL produced in *Escherichia coli* (loaded as a control), *lane 2*; proteins from the culture medium of cells transfected with the empty plasmid (pcDNA3.1) *lane 3*; proteins from the culture medium of cells transfected with the plasmid containing the 16K hPRL gene (pcDNA3.1-16K hPRL). The band corresponding to 16K hPRL is indicated. **(b)** Analysis of glycosylation. *Lane 4*; 30 ng recombinant 16K hPRL produced in *Escherichia coli* (loaded as a control), *lane 5*; proteins from the culture medium of cells transfected with plasmid pcDNA3.1-16K hPRL; *lane 6*; deglycosylated proteins from the culture medium of cells transfected with plasmid pcDNA3.1-16K hPRL. Culture medium of pcDNA3.1-16K hPRL-liposome-transfected 293T cells was incubated or not with N-glycosidase and subjected to western blotting as in **a**. The band corresponding to 16K hPRL is indicated.

**Figure 3** Reduction of B16-F10 melanoma growth by 16K hPRL. **(a)** C57BL/6J mice were subcutaneously inoculated with  $10^5$  B16F10 cells. After 3 days, the mice were treated with either pcDNA3.1-liposome complexes or pcDNA3.1-16K hPRL-liposome complexes. The complexes were injected peritumorally every 3 to 4 days. Each point represents the mean tumor volume in a group of mice. Error bars represent standard deviations. **(b)** Tumor volumes in mice at the end of the assay. Horizontal lines indicate the median tumor volume.

**Figure 4** Measurement of the level of 16K hPRL mRNA in B16F10 tumors by qRT PCR. RNA was extracted from tumors treated with lipoplexes composed of cationic liposomes and pcDNA3.1 or pcDNA3.1-16K hPRL. Transcript levels were analyzed by qRT-PCR. Data were normalized by quantification of cyclophilin B transcripts and are representative of three distinct experiments. Each bar represents the mean  $\pm$  SD, n=3.

**Figure 5** 16K hPRL reduces the vessel area in tumors. **(a)** Representative photographs of sections of tumors treated with pcDNA3.1-liposome complexes or with pcDNA3.1-16K

hPRL-liposome complexes by inoculation into mice. The sections are stained with anti-CD31 to reveal blood vessels (red) (x100 magnification). **(b)** The mean vessel density  $\pm$  SEM was determined on CD31-positive vessels in x100 power fields of each section as described under Materials and Methods. **(c)** Total vessel area  $\pm$  SEM was determined on CD31-positive vessels in x100 power fields of each section as described under Materials and Methods. **(d)** The average vessels size  $\pm$  SEM was determined on CD31-positive vessels in x100 power fields of each section as described under Materials and Methods. **(e)** The size distribution  $\pm$  SEM was determined on CD31-positive vessels in x100 power fields of each section as described under Materials and Methods.

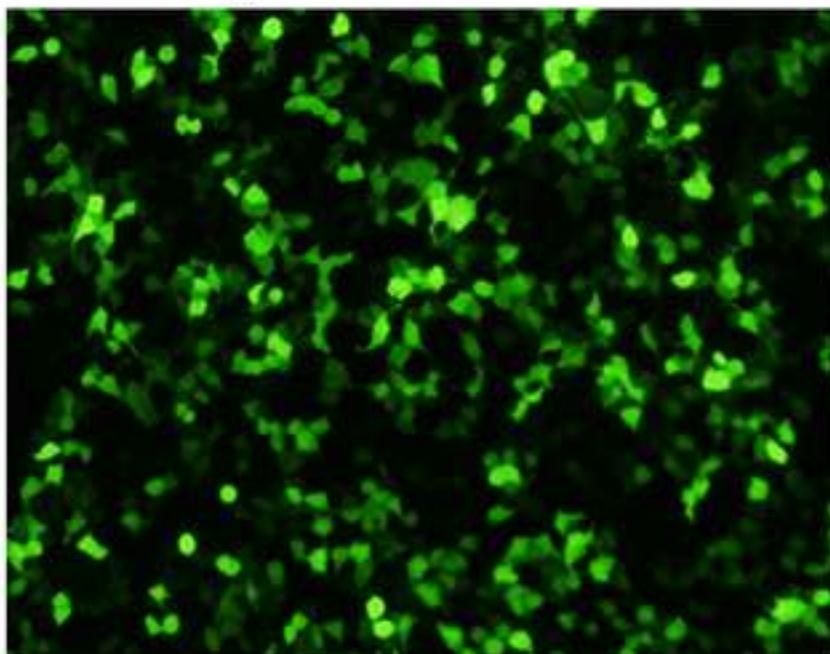


## Bibliography

- [1] P. Carmeliet, Angiogenesis in life, disease and medicine, *Nature* 438 (2005) 932-936.
- [2] A. Tandle, D.G. Blazer, 3rd, S.K. Libutti, Antiangiogenic gene therapy of cancer: recent developments, *J Transl Med* 2 (2004) 22.
- [3] G. Bergers, L.E. Benjamin, Tumorigenesis and the angiogenic switch, *Nat Rev Cancer* 3 (2003) 401-410.
- [4] J. Folkman, Endogenous angiogenesis inhibitors, *Apmis* 112 (2004) 496-507.
- [5] N. Ferrara, C. Clapp, R. Weiner, The 16K fragment of prolactin specifically inhibits basal or fibroblast growth factor stimulated growth of capillary endothelial cells, *Endocrinology* 129 (1991) 896-900.
- [6] G. D'Angelo, I. Struman, J. Martial, R.I. Weiner, Activation of mitogen-activated protein kinases by vascular endothelial growth factor and basic fibroblast growth factor in capillary endothelial cells is inhibited by the antiangiogenic factor 16-kDa N-terminal fragment of prolactin, *Proc Natl Acad Sci U S A* 92 (1995) 6374-6378.
- [7] G. D'Angelo, J.F. Martini, T. Iiri, W.J. Fantl, J. Martial, R.I. Weiner, 16K human prolactin inhibits vascular endothelial growth factor-induced activation of Ras in capillary endothelial cells, *Mol Endocrinol* 13 (1999) 692-704.
- [8] H. Lee, I. Struman, C. Clapp, J. Martial, R.I. Weiner, Inhibition of urokinase activity by the antiangiogenic factor 16K prolactin: activation of plasminogen activator inhibitor 1 expression, *Endocrinology* 139 (1998) 3696-3703.
- [9] J.F. Martini, C. Piot, L.M. Humeau, I. Struman, J.A. Martial, R.I. Weiner, The antiangiogenic factor 16K PRL induces programmed cell death in endothelial cells by caspase activation, *Mol Endocrinol* 14 (2000) 1536-1549.
- [10] S.P. Tabruyn, C.M. Sorlet, F. Rentier-Delrue, V. Bours, R.I. Weiner, J.A. Martial, I. Struman, The antiangiogenic factor 16K human prolactin induces caspase-dependent apoptosis by a mechanism that requires activation of nuclear factor-kappaB, *Mol Endocrinol* 17 (2003) 1815-1823.
- [11] S.P. Tabruyn, C. Sabatel, N.Q. Nguyen, C. Verhaeghe, K. Castermans, L. Malvaux, A.W. Griffioen, J.A. Martial, I. Struman, The angiostatic 16K human prolactin overcomes endothelial cell anergy and promotes leukocyte infiltration via nuclear factor-kappaB activation, *Mol Endocrinol* 21 (2007) 1422-1429.
- [12] C. Clapp, J.A. Martial, R.C. Guzman, F. Rentier-Delure, R.I. Weiner, The 16-kilodalton N-terminal fragment of human prolactin is a potent inhibitor of angiogenesis, *Endocrinology* 133 (1993) 1292-1299.
- [13] D. Hilfiker-Kleiner, K. Kaminski, E. Podewski, T. Bonda, A. Schaefer, K. Sliwa, O. Forster, A. Quint, U. Landmesser, C. Doerries, M. Luchtefeld, V. Poli, M.D. Schneider, J.L. Balligand, F. Desjardins, A. Ansari, I. Struman, N.Q. Nguyen, N.H. Zschemisch, G. Klein, G. Heusch, R. Schulz, A. Hilfiker, H. Drexler, A cathepsin D-cleaved 16 kDa form of prolactin mediates postpartum cardiomyopathy, *Cell* 128 (2007) 589-600.
- [14] F. Bentzien, I. Struman, J.F. Martini, J. Martial, R. Weiner, Expression of the antiangiogenic factor 16K hPRL in human HCT116 colon cancer cells inhibits tumor growth in Rag1(-/-) mice, *Cancer Res* 61 (2001) 7356-7362.
- [15] J. Kim, W. Luo, D.T. Chen, K. Earley, J. Tunstead, L.Y. Yu-Lee, S.H. Lin, Antitumor activity of the 16-kDa prolactin fragment in prostate cancer, *Cancer Res* 63 (2003) 386-393.
- [16] N.Q. Nguyen, A. Cornet, S. Blacher, S.P. Tabruyn, J.M. Foidart, A. Noel, J.A. Martial, I. Struman, Inhibition of tumor growth and metastasis establishment by

- adenovirus-mediated gene transfer delivery of the antiangiogenic factor 16K hPRL, *Mol Ther* 15 (2007) 2094-2100.
- [17] Y. Cao, Endogenous angiogenesis inhibitors and their therapeutic implications, *Int J Biochem Cell Biol* 33 (2001) 357-369.
- [18] G. Thurston, J.W. McLean, M. Rizen, P. Baluk, A. Haskell, T.J. Murphy, D. Hanahan, D.M. McDonald, Cationic liposomes target angiogenic endothelial cells in tumors and chronic inflammation in mice, *J Clin Invest* 101 (1998) 1401-1413.
- [19] H. Maeda, J. Wu, T. Sawa, Y. Matsumura, K. Hori, Tumor vascular permeability and the EPR effect in macromolecular therapeutics: a review, *J Control Release* 65 (2000) 271-284.
- [20] K.S. Kim, H.S. Kim, J.S. Park, Y.G. Kwon, Y.S. Park, Inhibition of B16BL6 tumor progression by coadministration of recombinant angiostatin K1-3 and endostatin genes with cationic liposomes, *Cancer Gene Ther* 11 (2004) 441-449.
- [21] S.I. Kim, K.S. Kim, H.S. Kim, D.S. Kim, Y. Jang, K.H. Chung, Y.S. Park, Inhibitory effect of the salmosin gene transferred by cationic liposomes on the progression of B16BL6 tumors, *Cancer Res* 63 (2003) 6458-6462.
- [22] Y. Katanasaka, T. Ida, T. Asai, N. Maeda, N. Oku, Effective delivery of an angiogenesis inhibitor by neovessel-targeted liposomes, *Int J Pharm* 360 (2008) 219-224.
- [23] H. Pan, N.Q. Nguyen, H. Yoshida, F. Bentzien, L.C. Shaw, F. Rentier-Delrue, J.A. Martial, R. Weiner, I. Struman, M.B. Grant, Molecular targeting of antiangiogenic factor 16K hPRL inhibits oxygen-induced retinopathy in mice, *Invest Ophthalmol Vis Sci* 45 (2004) 2413-2419.
- [24] J. Folkman, Tumor angiogenesis: therapeutic implications, *N Engl J Med* 285 (1971) 1182-1186.
- [25] N. Bouck, V. Stellmach, S.C. Hsu, How tumors become angiogenic, *Adv Cancer Res* 69 (1996) 135-174.
- [26] Q.R. Chen, D. Kumar, S.A. Stass, A.J. Mixson, Liposomes complexed to plasmids encoding angiostatin and endostatin inhibit breast cancer in nude mice, *Cancer Res* 59 (1999) 3308-3312.
- [27] M. Rodolfo, E.M. Cato, S. Soldati, R. Ceruti, M. Asioli, E. Scanziani, P. Vezzoni, G. Parmiani, M.G. Sacco, Growth of human melanoma xenografts is suppressed by systemic angiostatin gene therapy, *Cancer Gene Ther* 8 (2001) 491-496.
- [28] C. Gonzalez, A.M. Corbacho, J.P. Eiserich, C. Garcia, F. Lopez-Barrera, V. Morales-Tlalpan, A. Barajas-Espinosa, M. Diaz-Munoz, R. Rubio, S.H. Lin, G. Martinez de la Escalera, C. Clapp, 16K-prolactin inhibits activation of endothelial nitric oxide synthase, intracellular calcium mobilization, and endothelium-dependent vasorelaxation, *Endocrinology* 145 (2004) 5714-5722.

**Lipofectamine**



**Cationic lipoplexes**

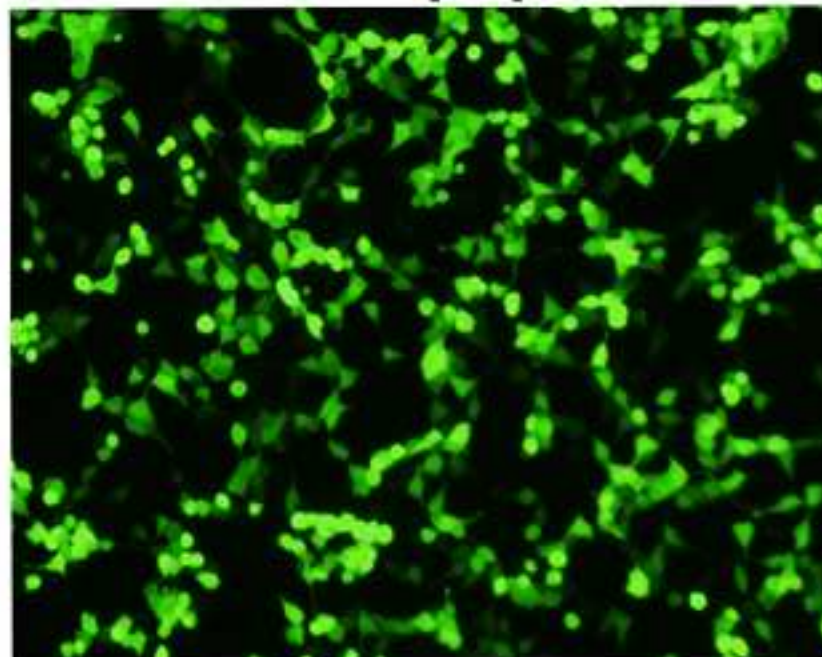


Figure 2  
[Click here to download high resolution image](#)

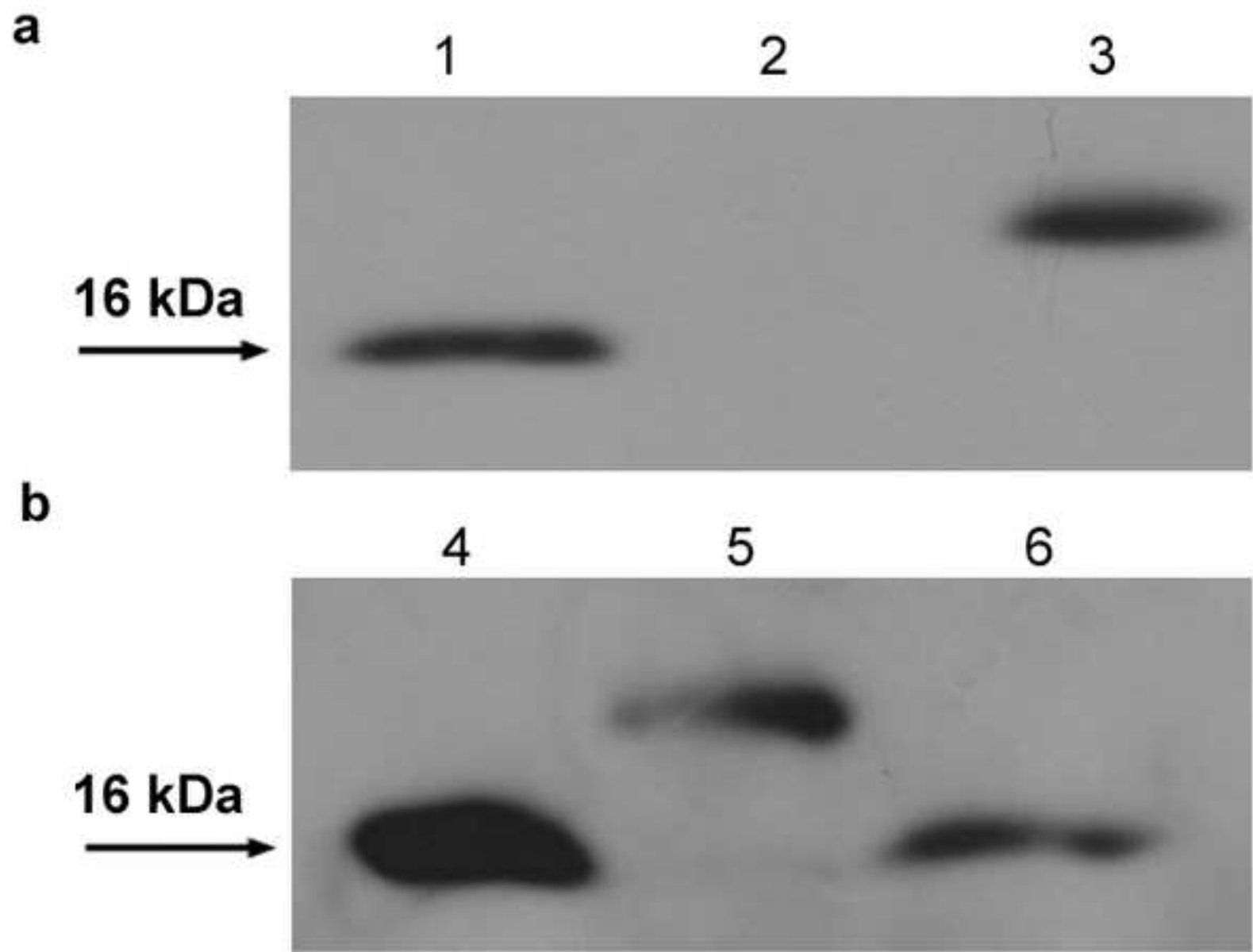


Figure 3  
[Click here to download high resolution image](#)

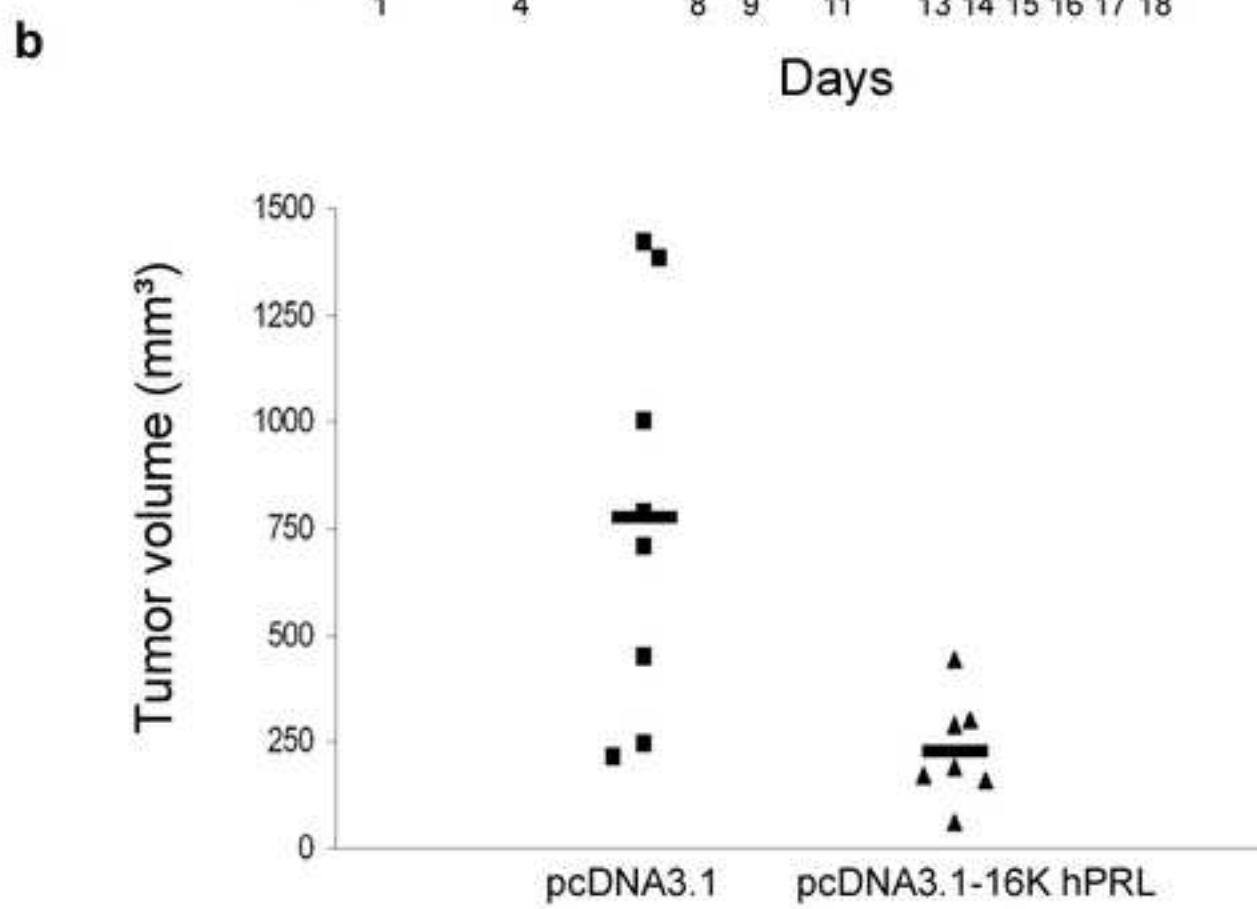
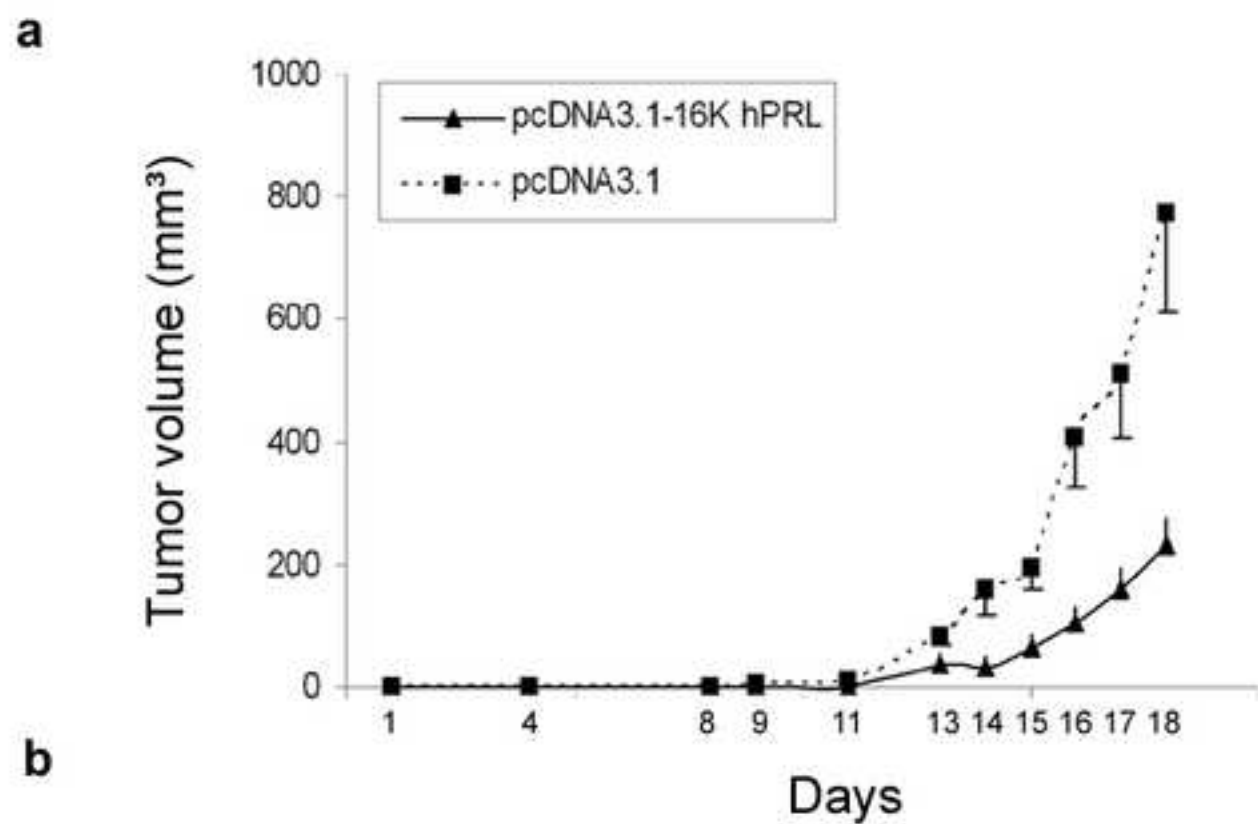
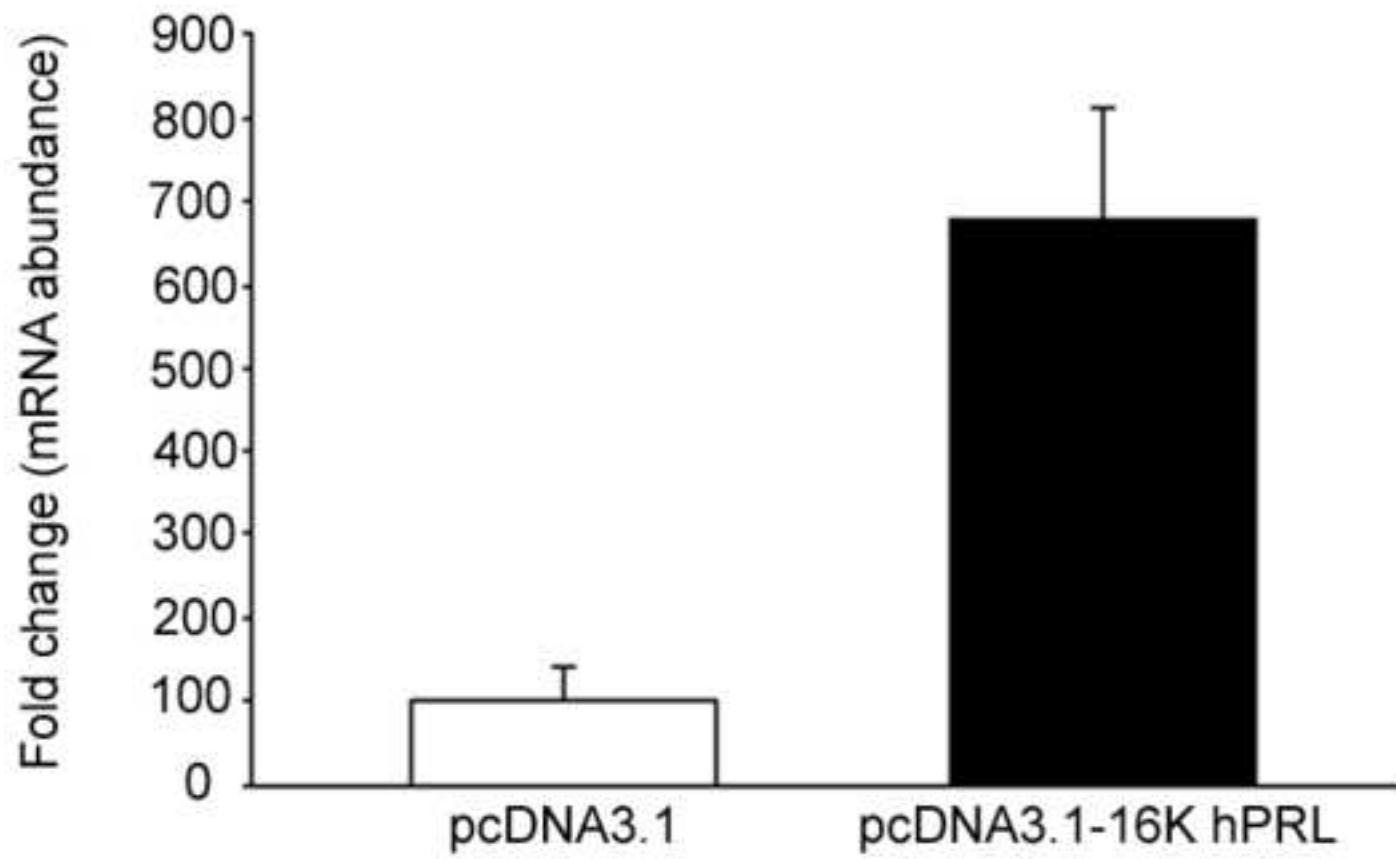


Figure 4  
[Click here to download high resolution image](#)



**Figure 5**  
[Click here to download high resolution image](#)

